A Journal of the Gesellschaft Deutscher Chemiker

Angewandte International Edition GDCh Chemie

www.angewandte.org

Accepted Article

Title: Strategic Design of Catalytic Lysine-Targeting Reversible Covalent BCR-ABL Inhibitors

Authors: David Quach, Guanghui Tang, Jothi Anantharajan, Nithya Baburajendran, Anders Poulsen, John Wee, Priya Retna, Rong Li, Boping Liu, Doris Tee, Perlyn Kwek, Joma Joy, Wang-Qi Yang, Chong-Jing Zhang, Klement Foo, Thomas Keller, and Shao Q. Yao

To be cited as: *Angew. Chem. Int. Ed.* 10.1002/anie.202105383

Link to VoR: https://doi.org/10.1002/anie.202105383

WILEY-VCH

10.1002/anie.202105383

WILEY-VCH

RESEARCH ARTICLE

Strategic Design of Catalytic Lysine-Targeting Reversible Covalent BCR-ABL Inhibitors

David Quach,[a][b] Guanghui Tang,[c] Jothi Anantharajan,[b] Nithya Baburajendran,[b] Anders Poulsen,[b] John L. K. Wee,[b] Priya Retna,[b] Rong Li,[b] Boping Liu,[b] Doris H. Y. Tee,[b] Perlyn Z. Kwek,[b] Joma K. Joy,[b] Wan-Qi Yang,[d] Chong-Jing Zhang,[d] Klement Foo,*[b] Thomas H. Keller,*[b] Shao Q. Yao*[a][c]

[a] Dr. D. Quach, Prof. Dr. S. Q. Yao
NUS Graduate School for Integrative Sciences and Engineering, 21 Lower Kent Ridge, University Hall, Tan China Tuan Wing, #04-02, Singapore 119077
E-mail: chmyaosq@nus.edu.sg
[b] Dr. D. Quach, Dr. J. Anantharajan, Dr. N. Baburajendran, Dr. A. Poulsen, J. L. K. Wee, P. Retna, R. Li, B. Liu, D. H. Y. Tee, P. Z. Kwek, Dr. J. K. Joy, Dr. K. Foo, Dr. T. H. Keller
Experimental Drug Development Centre, 10 Biopolis Road, Chromos, #05-01, Singapore 138670
E-mail: thkeller@eddc.a-star.edu.sg, klementfoo@gmail.com
[c] Dr. G. Tang, Prof. Dr. S. Q. Yao
Department of Chemistry, National University of Singapore, Singapore 117543
[d] W-.Q. Yang, Dr. C-.J. Zhang
State Key Laboratory of Bioactive Substances and Functions of Natural Medicines and Beijing Key Laboratory of Active Substances Discovery and Druggability Evaluation, Institute of Materia Medica Peking Union Medical College and Chinese Academy of Medical Sciences, Beijing, China, 100050

Supporting information for this article is given via a link at the end of the document.

Abstract: Targeted covalent inhibitors have re-emerged as validated drugs to overcome acquired resistance in cancer treatment. Herein, by using a carbonyl boronic acid (CBA) warhead, we report the structure-based design of BCR-ABL inhibitors via reversible covalent targeting of the catalytic lysine with improved potency against both wild-type and mutant ABL kinases, especially ABL^{T315I} bearing the gatekeeper residue mutation. We show the evolutionarily conserved lysine can be targeted selectively, and the selectivity depends largely on molecular recognition of the non-covalent pharmacophore in this class of inhibitors, probably due to the moderate reactivity of the warhead. We report the first co-crystal structures of covalent inhibitor-ABL kinase domain complexes, providing insights into the interaction of this warhead with the catalytic lysine. We also employed label-free mass spectrometry to evaluate off-targets of our compounds at proteome-wide level in different mammalian cells.

Introduction

Chronic myeloid leukemia (CML) arises from a genetic abnormality in human chromosome 22, which is unusually short and defective because of the reciprocal translocation of genetic material from chromosome 9.[1] Gene expression leads to the formation of a constitutively active BCR-ABL1 kinase, which aberrantly activates multiple signaling pathways that bring about uncontrollable cell growth and differentiation.[2] Despite the clinical success of ATP-competitive inhibitors,[3] a significant number of patients have suffered from relapse due to drug resistance, which can arise from point mutations that severely reduce the effect of such inhibitors.[4,5] An important mutant in CML is BCR-ABL^{T315I} which can only be inhibited by ponatinib (Iclusig).[6] Targeted covalent

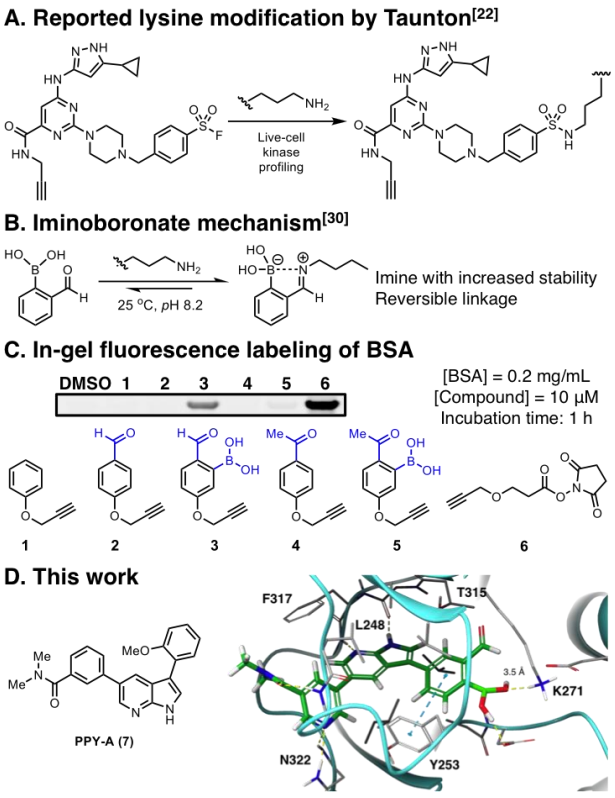

Figure 1. (A) A previously reported sulfonyl fluoride probe for covalent lysine labeling of kinases in live cells.[22] (B) Lysine modification based on the formation of a stable iminoboronate with 2-formylbenzene boronic acid.[30] (C) Model study of various lysine-targeting probes by using bovine serum albumin (BSA). (D) Structure-based design of a BCR-ABL inhibitor (**12**) targeting the catalytic lysine K271, based on the previously reported inhibitor PPY-A (**7**).[32]

10.1002/anie.202105383

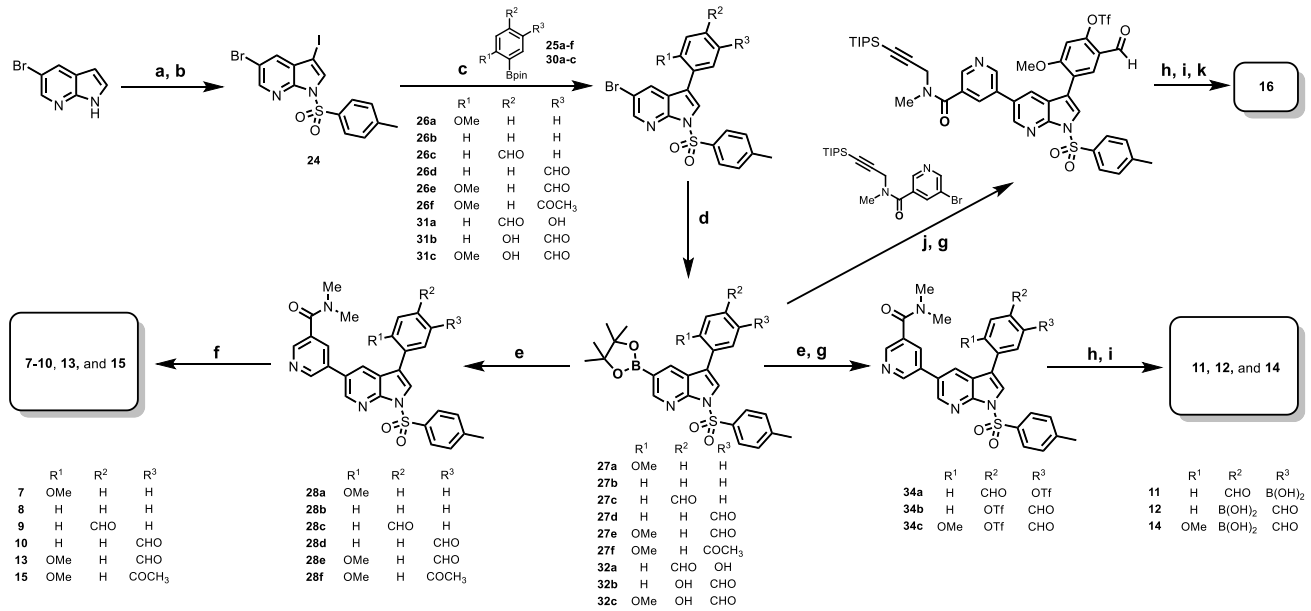

Scheme 1. Synthesis of key inhibitors used in this work. (a) NIS, acetone, rt, 1 h, 98%; (b) TsCl, NaH, THF, 0 °C, 3 h, 96%; (c) Pd(dppf)Cl_2, K_2CO_3, 1,4-dioxane/H_2O (9:1), 70 °C, 7 h, 60-80%; (d) B_2pin_2, Pd(dppf)Cl_2, KOAc, 1,4-dioxane, 100 °C, 7 h, 70-90%; (e) 5-bromo-*N*,*N*-dimethylnicotinamide, Pd(dppf)Cl_2, K_2CO_3, 1,4-dioxane/H_2O (9:1), 95 °C, 7 h, 70-80%; (f) LiOH, MeOH/dioxane/H_2O (2:2:1), rt, 1 h, 80-90%; (g) CF_3SO_2Cl, K_2CO_3, DMF, rt, 2-4 h, 80-90%; (h) B_2pin_2, Pd(dppf)Cl_2, KOAc, 1,4-dioxane, 100 °C, 7 h; (i) Cs_2CO_3, THF/MeOH (2:1), 40-50 °C, 1 h, 10-20% (2-step yields from (h) and (i)); (j) 5-bromo-*N*-methyl-*N*-(3-(triisopropylsilyl)prop-2-yn-1-yl)nicotinamide, Pd(dppf)Cl_2, K_2CO_3, 1,4-dioxane/H_2O (9:1), 95 °C, 7 h, 80-90%; (k) TBAF, THF/H_2O, rt, 2.5% (3-step yield from (h), (i) and (k)).

inhibitors offer advantages such as greater potency and prolonged duration of action over non-covalent inhibitors, and they have re-emerged in recent years as demonstrated by the clinical success of, for example, osimertinib.[7-11] The standard strategy to design irreversible kinase inhibitors uses Michael acceptors to target poorly conserved cysteine residues near the active site of kinases.[12] This was thought to provide a measure of selectivity; however, Cravatt and coworkers have demonstrated that even carefully designed cysteine-targeting covalent inhibitors have off-target effects.[13] Furthermore, resistance mechanisms including cysteine point mutations ($EGFR^{C797S}$ and BTK^{C481S}) often render cysteine-targeting covalent drugs ineffective.[11] To our knowledge, no covalent drugs against any of the known BCR-ABL mutants have been reported up to date due to a lack of targetable cysteine residues.[14]

Since the catalytic lysine residue is essential for the enzymatic activity of all protein kinases and therefore, considered less prone to mutation,[15,16] we have been interested to study this evolutionarily conserved residue in the ATP pocket with the aim to produce covalent kinase inhibitors as an alternative strategy in drug design. Many non-selective lysine-modifying probes, including the use of sulfonyl fluorides and activated esters, have been reported.[17-23] Taunton and co-workers recently reported sulfonyl fluoride-containing probes for lysine-targeting in kinases (Figure 1A).[22] Campos et al later identified lysine-targeting kinase inhibitors that used an activated ester.[23] Since cellular toxicity is a major concern for both tool compounds and drug candidates, many research groups aspire to tune the reactivity of covalent warheads.[24-28] For example, Taunton and co-workers used electron-deficient Michael acceptors for the design of cysteine-targeting reversible covalent kinase inhibitors.[29] Carbonyl boronic acids (CBAs) have recently been shown to reversibly but covalently modify amino groups in proteins (Figure 1B);[30] however, this chemistry, to the best of our knowledge, has not been used to develop covalent kinase inhibitors.[31] Our aim was therefore to design reversible, covalent inhibitors targeting the catalytic lysine residue in kinases as a general approach to combat drug resistance. We report herein the first successful examples of lysine-targeting reversible covalent kinase inhibitors based on CBAs and the corresponding iminoboronate chemistry (Figure 1C/D); our results showed that such compounds possessed potent and long-lasting inhibition against BCR-ABL wild type and mutants by targeting the catalytic lysine residue K271 in this kinase.

Results and Discussion

At the outset, a mechanistic study was carried out to compare the relative reactivity of model probes **3** and **5** with an NHS probe (**6**) and other controls by using BSA as reference in the presence of a rhodamine-azide "click" reporter (Figure 1C). Removal of either carbonyl or boronic acid (or both; e.g. **1**, **2** and **4**) caused complete abolishment in fluorescent labeling of BSA in

Table 1. Compounds **7-16** in the Biochemical Assay against ABL^{WT}, ABL^{T315I} and ABL^{E255K}.

	Compound	R^1	R^2	R^3	IC_{50} (WT) (nM)			IC_{50} (T315I) (nM)		IC_{50} (E255K) (nM)	
					T = 0 h	T = 0.25 h	T = 12 h	T = 0 h	T = 12 h	T = 0 h	T = 12 h
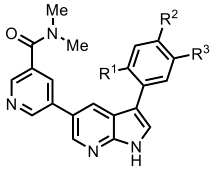 7-16	**7**	OMe	H	H	2.0 ± 0.1	2.0 ± 0.2	2.0 ± 0.1	1.0 ± 0.1	1.0 ± 0.1	9.0 ± 0.5	10.0 ± 0.4
	8	H	H	H	-	43 ± 5	-	-	-	-	-
	9	H	CHO	H	-	75 ± 3	-	-	-	-	-
	10	H	H	CHO	7.0 ± 0.3	8.0 ± 0.1	-	-	-	-	-
	11	H	CHO	$B(OH)_2$	-	414 ± 18	52 ± 2	-	-	-	-
	12	H	$B(OH)_2$	CHO	83 ± 2	59 ± 1	5.0 ± 0.4	-	-	-	-
	13	OMe	H	CHO	3.0 ± 0.1	3.0 ± 0.2	3.0 ± 0.1	4.0 ± 0.2	3.0 ± 0.1	9.0 ± 0.1	8.0 ± 0.1
	14	OMe	$B(OH)_2$	CHO	13.0 ± 0.3	12.0 ± 0.4	1.7 ± 0.2	25 ± 1	0.50 ± 0.02	43 ± 2	0.50 ± 0.03
	15	OMe	H	$COCH_3$	-	7.0 ± 0.3	-	-	-	-	-
	16	OMe	$B(OH)_2$	CHO	-	10.0 ± 0.4	-	-	-	-	-

3 and **5**. Between **3** and **5**, the former consistently labeled BSA more strongly, indicating the aldehyde was more reactive than the ketone. As expected, both **3** and **5** produced much weaker fluorescence labeling of BSA compared to **6**, suggesting CBAs have attenuated lysine reactivity compared to the highly reactive NHS-based irreversible lysine modifier.[18] We next designed suitable CBA-containing BCR-ABL kinase inhibitors (Figure 1D). Molecular modeling studies were first carried out by incorporating a CBA warhead into the previously reported ABL1 inhibitor PPY-A (**7**) (PDB ID: 2QOH);[32] results showed that introducing the required functionality would not disrupt the binding to the protein, and with the distance between the proposed CBA moiety and the highly flexible catalytic lysine K271 being ~3.5 Å, formation of an iminoboronate in the kinase/inhibitor complex was indeed possible.

A library of analogs was synthesized in order to establish structure-activity relationship (Scheme 1, Table 1). The synthesis of a common intermediate **24** was done in two steps via iodination and tosylation of 5-bromoazaindole. **7**-**10** were obtained in four steps via Suzuki-Miyaura coupling reactions involving **24** to generate **26a**-**d**, which underwent Miyaura borylation that led to **27a**-**d**. The Suzuki-Miyaura cross coupling reaction was performed at a lower temperature of 60 °C in order to chemoselectively differentiate Br and I. **27a**-**d** then underwent a second Suzuki-Miyaura coupling reaction with 5-bromo-*N*,*N*-dimethylnicotinamide followed by subsequent removal of tosyl group with LiOH, leading to the formation of the desired inhibitors (**7**-**10**). The synthesis of CBA inhibitors **11** and **12** occured via a different route in which an additional step involving the conversion of OH to OTf, led to intermediates **34a** and **34b**; CF_3SO_2Cl and K_2CO_3 were shown to be the optimal choice. Other electrophiles such as $PhNTf_2$ and $(CF_3SO_2)_2O$ in the presence of bases such as triethylamine, NaH and pyridine did not work well despite heating. **34a** and **34b** underwent borylation and subsequent deprotection of the tosyl group by using Cs_2CO_3 was carried out to generate covalent inhibitors **11** and **12**.

By using a mobility shift assay based on Caliper's microfluidics capillary electrophoresis, the IC_{50} value of PPY-A (**7**) against wildtype ABL was determined to be 2 nM after 15 minutes of incubation (Table 1, Figure S1). Removal of the *o*-methoxy group reduced the potency by 20 folds (compound **8**). Introduction of *m*-aldehyde (compound **10**), however, improved the IC_{50} to 8.0 nM. Shifting the aldehyde functional group to the *para* position was not tolerated (compound **9**). Introduction of a boronic acid functionality led to inhibitors **11** and **12**. Simialr to **9** and **10**, **11** was about 10-fold less potent than **12** and therefore, the position of the aldehyde functional group played an important role in the inhibitory activity. As expected of covalent inhibitors, the enzyme inhibition of compound **12** improved from 83 nM (T = 0 h) to 5.0 nM (T = 12 h) as the incubation time was increased (Figure S2). Compound **10** did not show time-dependence of the IC_{50}, suggesting that the presence of the boronic acid in **12** may have led to the formation of an iminoboronate.[33]

To determine whether **12** was selective towards the catalytic lysine in ABL, mass spectrometric analysis was performed. MALDI-TOF analysis suggested that a single lysine-modified covalent adduct was formed with an observed *m/z* of 33156.38 Da (Figure 2A bottom; compared to calculated mass of 33156.59 Da). The reaction did not reach completion regardless of the concentration (up to 1 mM) and incubation time (up to 24 h) of **12**, indicating that an equilibrium was established.[30,31] On the other hand, incubating the ABL kinase domain with **10** of the same concentration did not lead to the formation of any detectable adduct, indicating again that the imine formation between **10** and ABL kinase domain, in the absence of boronic, cannot be detected in our experimental setup compared to a control using DMSO (Figure 2A top & Figure S3). Since the OMe group in **7** was important for ABL inhibition, the same functionality was added to **12**, providing compound **14** which was synthesized via a similar route (Scheme 1). As expected, **14** showed time-dependent IC_{50} values against ABL from 13 nM at 0 h to 1.7 nM after 12 h (Table 1, Figure S2); further testing of **7** and **14** against two ABL mutants indicated that **14**

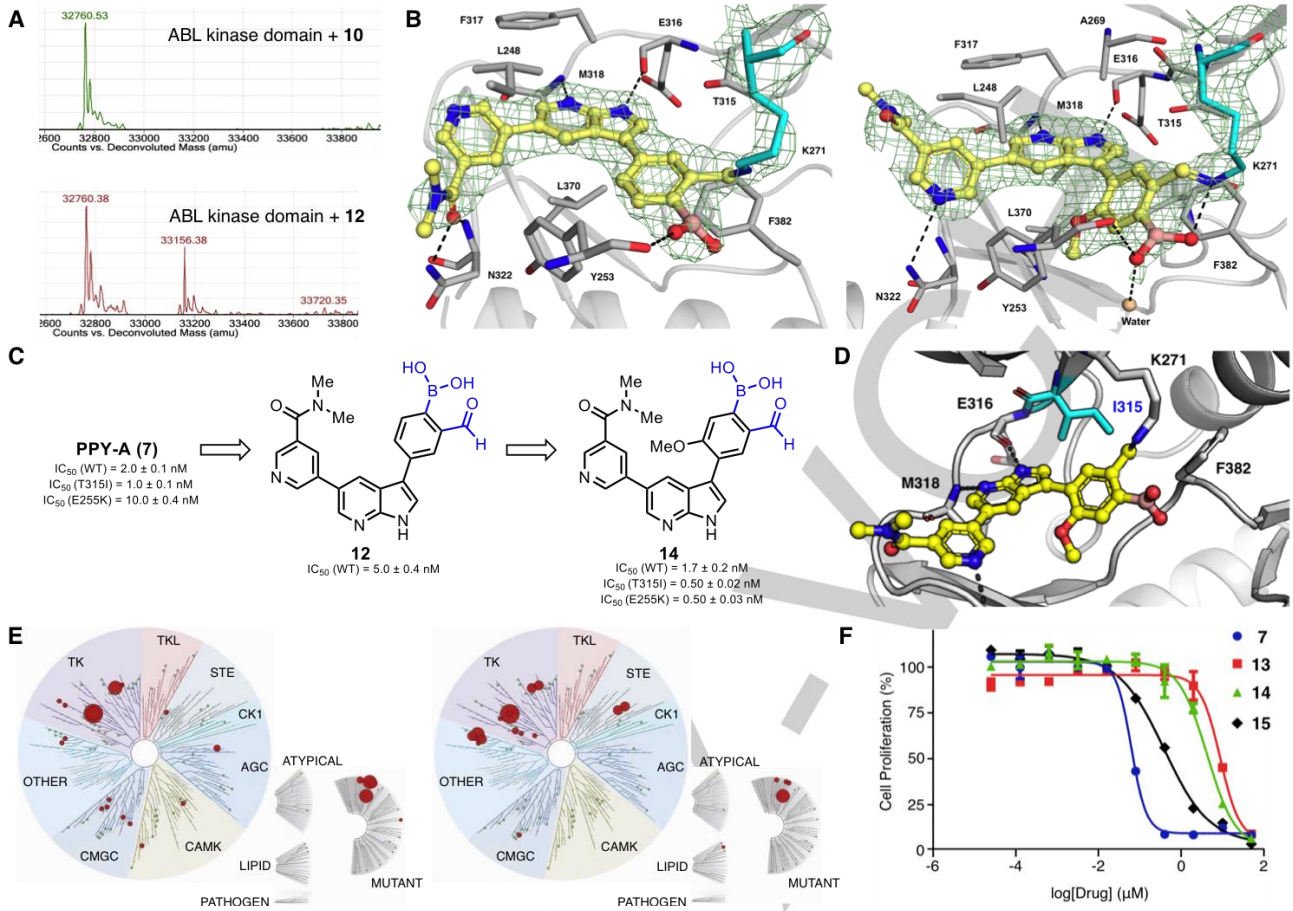

Figure 2. (A) Mass spectrometric analysis of the ABL kinase domain-**12** complex (bottom). (top): ABL kinase domain-**10** complex as control. (B) Cocrystal structures of the ABL kinase domain with **12** (left; PDB ID: 7CC2) and **14** (right; PDB ID: 7DT2) showing the composite omit map ($2F_o$-F_c) contoured to 1σ in green mesh. The front loop was removed for better visibility. (C) Comparison of ABL inhibition (WT and mutants) of PPY-A (**7**), **12** and **14** after 12 h. See Table 1 and Figure S2 for details. (D) Modeled structure of ABL^{T315I} kinase domain-**14** complex based on the obtained cocrystal structure of ABL^{WT} kinase domain-**14** complex. (E) Dendrograms showing Kinome Scan™ of **7** (left) and **14** (right) at 1000 nM against 90 different kinases. (F) Anti-proliferative activity of **7**, **13**, **14** and **15** against K562 cells determined by CellTiter-Glo® viability assay.

showed time-dependent inhibition, with improved potency upon prolonged incubation, against both ABL^{T315I} and ABL^{E255K} when compared to **7** (Table 1, Figures 2C). In particular, **14** demonstrated an improved potency from 25 nM (T = 0 h) to 0.50 nM (T = 12 h) against ABL^{T315I} (50-fold improvement) and from 43 nM (T = 0 h) to 0.5 nM (T = 12 h) against ABL^{E255K} (100-fold improvement). The effect of point mutation on restricting access to the binding pocket or stabilizing certain protein conformations has been shown to adversely affect drug binding which tends to favor only a very specific target conformation;[10] however, our examples showed that targeting the catalytic lysine residues gave an advantage in this context.

The X-ray cocrystal structures of **12** and **14** with the ABL kinase domain (229-510) were solved up to 2.7 Å and 2.3 Å resolution, respectively, giving more insights into how this particular warhead interacts with the catalytic lysine residue (Figures 2B & S4-7; PDB IDs: 7CC2 and 7DT2); the continuous electron density from K271 in the ABL kinase domain to **12** and **14** suggests that the imine product was formed. We did not, however, observe the formation of the expected dative bond between the imine nitrogen and the boron atom. In fact, the lone pair of the imine appeared to be orientated away from the boron atom in both crystal structures. One of the reasons could be due to the vast structural difference between free small molecules and the macromolecule-inhibitor complex formed within the tight binding pocket of a protein target. The latter might have significantly influenced the orientation of the bound small molecule. Indeed, in a model experiment (Figure S8), we were able to show that an iminoboronate adduct could be successfully captured by ^{11}B NMR. Since the biochemical assays and the MALDI-TOF analysis suggested that the boronic acid plays an important role in the formation of the adduct, we propose that the obtained cocrystal structures had successfully captured the key intermediate during the formation of the iminoboronates. Given the fact that **14** was able to potently inhibit ABL^{T315I} while imatinib and second-generation kinase inhibitors such as nilotinib, dasatinib failed to do so,[32] we next rationalized this observation by using the newly obtained structural data (Figure 2D); by building a modeled structural complex

10.1002/anie.202105383

of **14** and ABL kinase domain in which the T315 residue was artificially changed to I315, we observed no steric clash upon inhibitor binding. Imatinib, nilotinib and dasatinib possess crucial elongated structures that are extended to the back cleft of the ATP binding pocket in ABL, and T315I point mutation was expected to restrict access to the hydrophobic region at the rear of this pocket.[32] This is not the case for **14** which does not have any substituent that occupies this pocket. Finally, **14** demonstrated better biochemical activity than that of **7** due to apparent covalent modification (Figure 2C),[34] and the incorporation of both boronic acid and aldehyde did not appear to cause any steric clash with the I315 residue.

The kinetic parameters of binding and inactivation were next determined to better understand the non-bonded interaction of **12** and **14** with the kinase (Figures S9-10).[34-36] Both known irreversible and slow-binding reversible models were used to fit our inhibition data, and results indicated that the latter was the more suitable one, truly reflecting the slow binding modes of our potent inhibitors. **14** had a smaller K_I compared to that of **12**, thus confirming the critical role of OMe in **14** for increased affinity between the inhibitor and the ABL kinase domain. The conclusion was further strengthened by time-dependent IC_{50} biochemical assays in which the incubation time against ABL^{WT} was fixed at 15 min for **7**, **12** and **14** (Table 1); **14** (IC_{50} = 12 nM) was shown to be about 5-fold more potent than **12** (IC_{50} = 59 nM).

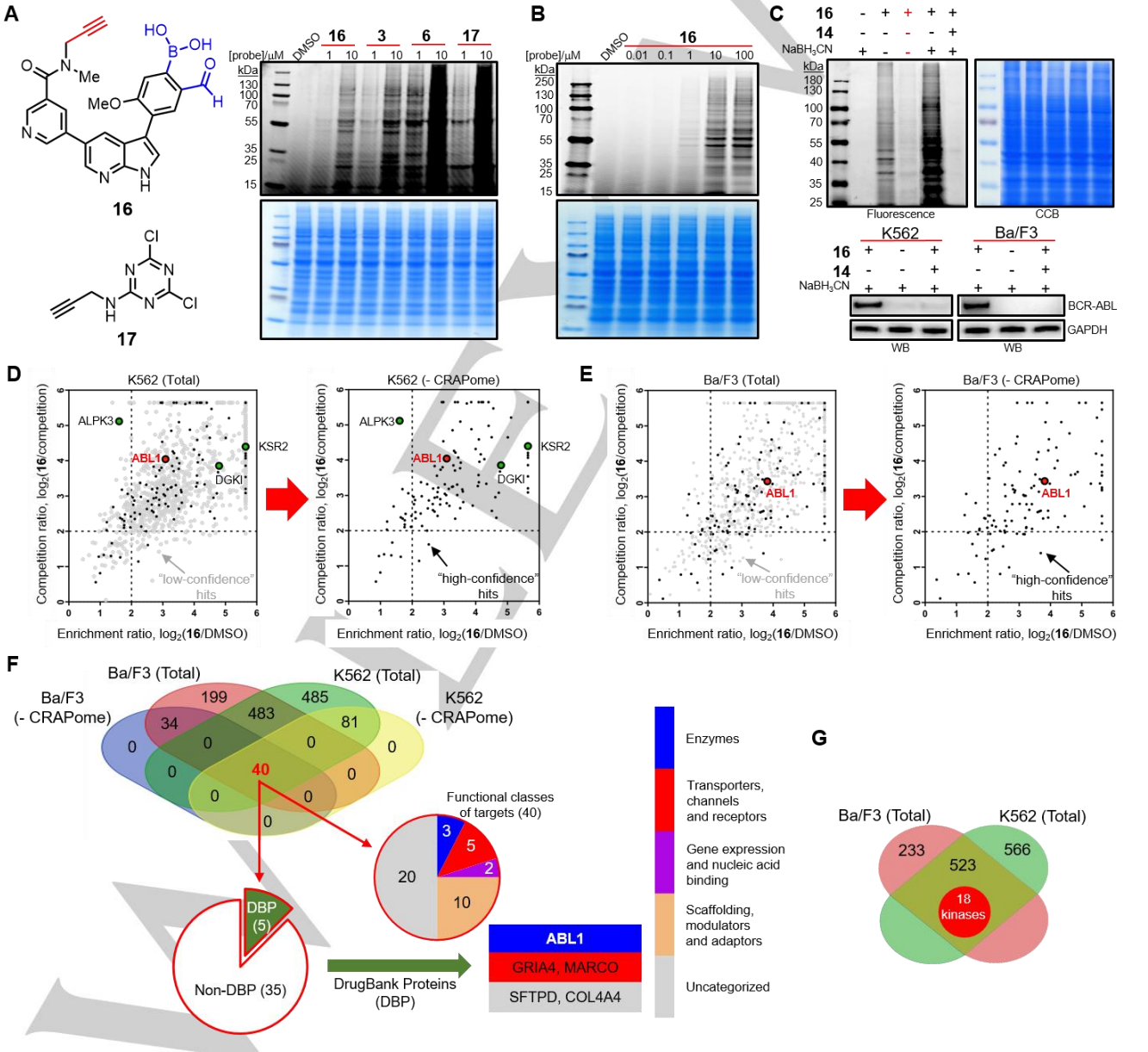

Figure 3. (A) Proteome reactivity profiles of compound **16** compared to **3**, **6** and **17** in K562 cell lysates (in PBS with 0.1% Triton, *p*H 7.5). (Top): in-gel fluorescence scanning; (Bottom): Coomassie staining (CBB). (B) Concentration-dependent proteomic reactivity profiles of **16** (0-100 μM) in Ba/F3 cells overexpressing $BCR\text{-}ABL^{WT}$. (C) Effect of washing by cold acetone and cold methanol (lane 4, highlighted in red; lane 3: no

washing) of probe-labeled K562 (see Figure S13 for corresponding Ba/F3 results) lysates in the absence and presence of excess $NaBH_3CN$ (top); (bottom) Western blotting (WB) detection of BCR-ABL^{WT} in lysates of both K562 and Ba/F3 cells following pull-down (PD) assays. GAPDH = loading control. [compound **16**] = 10 μM, and [compound **14**] = 500 μM. Incubation time = 1 h. (D/E) Scatter plots showing potential cellular targets of **16** from probe-treated K562 and Ba/F3 cell lysates, respectively. x-axis shows "Enrichment ratio" between **16**- and DMSO-treated samples. y-axis shows "Competition ratio" between **16**- and **14**-treated samples. Results were further filtered to provide 'high-confidence hits" (right graphs). (F) Data analysis of shared targets identified from chemoproteomic experiments in (D/E). The 40 shared "high-confidence hits" were highlighted in red and further analyzed. See Supporting Information for details. (G) Venn diagram showing the shared 523 targets (including 18 kinases) identified in both K562 and Ba/F3 cells.

One of the potential concerns for covalent inhibitors like **14**, which target a key amino acid in the active site of kinases, is the selectivity. We therefore carried out Kinome Scan™ with a panel of ~100 protein kinases (Figure 2E); results showed highly similar interaction maps for compounds **7** (left) and **14** (right), suggesting that the degree of compound selectivity largely depended on the initial step of molecular recognition presumably due to the moderately reactive 2-carbonyl boronic acid warhead in **14**. The conclusion was further strengthened by the selectivity scores (Table S4). To evaluate the anti-proliferative activity of this class of inhibitors, compounds **7** and **14**, as well as reference compounds **13** and **15** (boronic acid-free versions of **14**; see Table 1), were tested in K562 cells. As shown in Figure 2F, compound **7** showed GI_{50} of 0.114 μM whereas compounds **13**, **14** and **15** were less active with GI_{50} values of 3.85 μM, 1.19 μM and 0.384 μM, respectively. In an attempt to understand the loss of activity, the cell permeability of three compounds were tested (Tables S5 and S6); Compound **13** showed poor recovery rates which could be due to metabolism of the aldehyde functional group for this particular pharmacophore.[37] The 10-fold improvement in the anti-proliferative activity of its ketone counterpart (e.g. **15**; GI_{50} = 0.384 μM) suggests that the aldehyde might not be the optimal choice for this scaffold in the cellular systems, and a ketone could be a more appropriate option in future studies.

Finally, to evaluate the proteome-wide reactivity and potential off-targets of **14** in live mammalian cells, we synthesized its alkyne-containing analog (**16**; Scheme 1) and carried out large-scale chemoproteomic studies (Figures 3, S11).[38] We first compared the proteome reactivity of the aldehyde-boronic acid moiety to other well-known lysine-targeting functionalities by using lysates from K562 cells (Figure 3A);[17,18] in-gel fluorescence scanning analysis of probe-labeled lysates, followed by CuAAC with a rhodamine azide,[39] showed that **3** demonstrated better selectivity at both 1 μM and 10 μM when compared to **6** and **17** which are known lysine-reactive electrophiles, but was predictably less selective compared to the kinase-targeting **16**, suggesting that molecular recognition was the dominant factor for similar compounds that contain low-reactivity electrophiles such as CBAs.[40,41] In **16**-treated samples, we observed a concentration-dependent labeling of proteomes, with saturated fluorescence signals at ~10 μM of the probe (Figure 3B). We next repeated the labeling experiment in the presence of $NaBH_3CN$ which helped trap the reversible covalent iminoboronates into more stable amine adducts (Figure 3C); a concomitant increase in the fluorescence intensity of the **16**-labeled proteome was observed. In contrast, in the absence of $NaBH_3CN$, washing the **16**-labeled proteome with cold acetone and methanol significantly reduced or abolished the labeling (compare lanes 3 and 4). This thus confirms the reversibility of iminoboronate bond. Further evidence of this reversibility was obtained by using ^{1}H NMR upon dilution with a model complex between 2-formylphenyl boronic acid and Ac-Lys-NHMe (Figure S12). Upon further enrichment of the labeled proteomes by pull-down (PD) experiments followed by Western blotting (WB) analysis, we confirmed successful labeling of endogenous BCR-ABT^{WT} and BCR-ABL^{T315I} from both K562 and Ba/F3 cell lysates (Figure 3C bottom, Figure S11B). By using DMSO-treated and **14**-competed samples as controls, we next carried out large-scale LC-MS analysis (Figures 3D-G, S13-14) to identify potential off-targets of **16**.[22,38,39] Consistent with strong labeling shown by in-gel fluorescence scanning (Figure 3C), probe **16** captured a number of off-targets in addition to the expected BCR-ABL (highlighted in red circles in Figure 3D/E). By setting stringent criteria to remove non-specific binders (i.e. those shown in CRAPome;[42] See supporting Information for details) and identify only "high-confidence hits" (right graphs in Figure 3D/E), we sucessfully identified 40 putative targets of **14** (Figure 3F); upon further analysis, ABL1 emerged as the only kinase identified from our experiments in both cell lines. These results are consistent with our earlier Kinome Scan™ data of **14** (e.g. Figure 2E) and indicate its alkyne-containing analog **16** was a selective ABL-targeting probe. Interestingly in K562 but not in Ba/F3 cells, three additional kinases were identified as "high-confidence hits" (shown in green circles, Figure 3D). By lowering our data filter criteria to include all shared targets identified in both K562 and Ba/F3 cells (523 in total; see Figure 3G), including those that appear in CRAPome, we were able to further identify additional potential kinase off-targets (Figure S13).

Conclusion

In summary, we have successfully demonstrated, for the first time, that the catalytic lysine of ABL can be selectively targeted by inhibitors bearing a carbonyl boronic acid moiety, leading to a reversible covalent adduct. The incorporation of the two substituents required for covalent bond formation reduced the affinity to the ABL active site; however, the slow formation of the iminoboronate led to highly potent inhibitors of ABL kinase and its mutants. We also showed that the

carbonyl boronic acid, which is a low-reactivity electrophile, can be used to design highly selective kinase inhibitors by maximizing molecular recognition. Such compounds might be attractive tools for chemical biology studies given recent interests in the development of reversible covalent inhibitors,[29,31,43] but could also serve as potential drug candidates in cases where improved potency might be desirable once they are fully optimized. We have also employed label-free mass spectrometry to evaluate potential off-targets of our compounds at proteome-wide level in different mammalian cell lines. In addition to the expected target, we also identified a few additional kinases as well as some non-kinases as potnetial off-targets. Unlike protein kinases which have a known catalytic lysine residue in their kinase active sites, non-kinase targets possess solvent-exposed lysine residues, thus rendering them potentially susceptible to probe labeling.

Acknowledgements

Financial support was provided by the Synthetic Biology Research & Development Programme (SBP) of National Research Foundation (SBP-P4 and SBP-P8) for Shao Q. Yao, the National Medical Research Council (NMRC) via the Open Fund – Young Individual Research Grant for Klement Foo and by the Agency for Science, Technology and Research (A*STAR) via the A*STAR Graduate Scholarship (AGS) for David Quach. Financial support from CAMS Innovation Fund for Medical Sciences (CIFMS) (2017-I2M-4−005) of China is also acknowledged. The ABL protein construct and glycerol stock were prepared by Yvonne Y. W. Tan and Dario B. Heymann. We thank Zi Ye for support in MS data analysis.

Keywords: cancer • lysine • covalent • reversible • proteomics

[1] R. Kurzrock, J. U. Gutterman, M. Talpaz, *N. Engl. J. Med.* **1988**, *319*, 990−998.
[2] T. G. Lugo, A. M. Pendergast, A. J. Muller, O. N. Witte, *Science* **1990**, *247*, 1079−1082.
[3] E. Jabbour, H. Kantarjian, *Am. J. Hematol.* **2016**, *91*, 252−265.
[4] H. M. Kantarjian, M. Baccarani, E. Jabbour, G. Saglio, J. E. Cortes, *Clin. Cancer Res.* **2011**, *17*, 1674−1683.
[5] Z. Iqbal, A. Aleem, M. Iqbal, M. I. Naqvi, A. Gill, A. S. Taj, A. Qayyum, N. ur-Rehman, A. M. Khalid, I. H. Shah, M. Khalid, R. Haq, M. Khan, S. M. Baig, A. Jamil, M. N. Abbas, M. Absar, A. Mahmood, M. Rasool, T. Akhtar, *PLos One* **2013**, *8*, e55717.
[6] T. Anagnostou, M. R. Litzow, *Blood Lymphat. Cancer* **2017**, *2018*, 1−9.
[7] D. S. Johnson, E. Weerapana, B. F. Cravatt, *Future Med. Chem.* **2010**, *2*, 949−964.
[8] A. Chaikuad, P. Koch, S. A. Laufer, S. Knapp, *Angew. Chem. Int. Ed.* **2018**, 57, 4372−4385.
[9] Z. Zhao, P. E. Bourne, *Drug Discov. Today* **2018**, *23*, 727−735.
[10] J. Engel, J. Lategahn, D. Rauh, *ACS Med. Chem. Lett.* **2016**, *7*, 2−5.
[11] S-H. I. Ou, *Crit. Rev. Oncol. Hematol.* **2012**, *83*, 407−421.
[12] Q. S. Liu, Y. Sabnis, Z. Zhao, T. H. Zhang, S. J. Buhrlage, L. H. Jones, N. S. Gray, *Chem. Biol.* **2013**, *20*, 146−159.
[13] S. Niessen, M. M. Dix, S. Barbas, Z. E. Potter, S. Lu, O. Brodsky, S. Planken, D. Behenna, C. Almaden, K. S. Gajiwala, K. Ryan, R. Ferre, M. R. Lazear, M. M. Hayward, J. C. Kath, B. F. Cravatt, *Cell Chem. Bio.* **2017**, *24*, 1388−1400.
[14] F. Rossari, F. Minutolo, E. Orciuolo, *J. Hematol. Oncol.* **2018**, *11*, 1−14.
[15] A. C. Carrera, K. Alexandrov, T. M. Roberts, *Proc. Natl. Acad. Sci. U. S. A.* **1993**, *90*, 442−446.
[16] R. Liu, Z. Yue, C. C. Tsai, J. Shen, *J. Am. Chem. Soc.* **2019**, *141*, 6553−6560.
[17] D. A. Shannon, R. Banerjee, E. R. Webster, D. W. Bak, C. Wang, E. Weerapana, *J. Am. Chem. Soc.* **2014**, *136*, 3330−3333.
[18] C. C. Ward, J. L. Kleinman, D. K. Nomura, *ACS Chem. Biol.* **2017**, *12*, 1478−1483.
[19] A. Cuesta, J. Taunton, *Annu. Rev. Biochem.* **2019**, *88*, 365−381.
[20] M. Gehringer, S. A. Laufer, *J. Med. Chem.* **2019**, *62*, 5673−5724.
[21] S. M. Hacker, K. M. Backus, M. R. Lazear, S. Forli, B. E. Correia, B. F. Cravatt, *Nat. Chem.* **2017**, *9*, 1181−1190.
[22] Q. Zhao, X. Ouyang, X. Wan, K. S. Gajiwala, J. C. Kath, L. H. Jones, A. L. Burlingame, J. Taunton, *J. Am. Chem. Soc.* **2017**, *139*, 680−685.
[23] S. E. Dalton, L. Dittus, D. A. Thomas, M. A. Convery, J. Nunes, J. T. Bush, J. P. Evans, T. Werner, M. Bantscheff, J. A. Murphy, S. Campos, *J. Chem. Am. Soc.* **2018**, *140*, 932−939.
[24] U. P. Dahal, A. M. Gilbert, R. S. Obach, M. E. Flanagan, J. M. Chen, C. Garcia-Irizarry, J. T. Starr, B. Schuff, D. P. Uccello, J. A. Young, *Med. Chem. Commun.* **2016**, *7*, 864−872.
[25] J. Pettinger, K. Jones, M. D. Cheeseman, *Angew. Chem. Int. Ed.* **2017**, *56*, 15200−15209.
[26] P. Martín-Gago, C. A. Olsen, *Angew. Chem. Int. Ed.* **2019**, *58*, 957−966.
[27] L. H. Jones, *Angew. Chem. Int. Ed.* **2018**, *57*, 9220−9223.
[28] D. E. Mortenson, G. J. Brighty, L. Plate, G. Bare, W. Chen, S. Li, H. Wang, B. F. Cravatt, S. Forli, E. T. Powers, K. B. Sharpless, I. A. Wilson, J. W. Kelly, *J. Am. Chem. Soc.* **2018**, *140*, 200−210.
[29] I. M. Serafimova, M. A. Pufall, S. Krishnan, K. Duda, M. S. Cohen, R. L. Maglathlin, J. M. McFarland, R. M. Miller, M. Frödin, J. Taunton, *Nat. Chem. Biol.* **2012**, *8*, 471−476.
[30] S. Cambray, J. Gao, *Acc. Chem. Res.* **2018**, *51*, 2198-2206.
[31] G. Akçay, M. A. Belmonte, B. Aquila, C. Chuaqui, A.W. Hird, M. L. Lamb, P. B. Rawlins, N. Su, S. Tentarelli, N. P. Grimster, Q. Su, *Nat. Chem. Biol.* **2016**, *12*, 931−936.
[32] T. Zhou, L. Parillon, F. Li, Y. Wang, J. Keats, S. Lamore, Q. Xu, W. Shakespeare, D. Dalgarno, X. Zhu, *Chem. Biol. Drug Des.* **2007**, *70*, 171−181.
[33] P. M. S. D. Cal, J. B. Vicente, E. Pires, A. V. Coelho, L. F. Veiros, C. Cordeiro, P. M. P. Gois, *J. Am. Chem. Soc.* **2012**, *134*, 10299−10305.
[34] R. A. Bauer, *Drug Discov. Today* **2015**, *20*, 1061−1073.
[35] J. M. Bradshaw, J. M. McFarland, V. O. Paavilainen, A. Bisconte, D. Tam, V. T. Phan, S. Romanov, D. Finkle, J. Shu, V. Patel, T. Ton, X. Li, D. G. Loughhead, P. A. Nunn, D. E. Karr, M. E. Gerritsen, J. O. Funk, T. D. Owens, E. Verner, K. A. Brameld, R. J. Hill, D. M. Goldstein, J. Taunton, *Nat. Chem. Biol*. **2015**, *11*, 525−531.
[36] M. Goličnik, J. Stojan, *Biochem. Mol. Biol. Educ.* **2004**, *32*, 228−235.
[37] L. A. Admed, H. Younus, *Drug Metab. Rev.* **2019**, *51*, 42−64.
[38] B. R. Lanning, L. R. Whitby, M. M. Dix, J. Douhan, A. M. Gilbert, E. C. Hett, T. O. Johnson, C. Joslyn, J. C. Kath, S. Niessen, L. R. Roberts, M. E. Schnute, C. Wang, J. J. Hulce, B. Wei, L. O. Whiteley, M. M. Hayward, B. F. Cravatt, *Nat. Chem. Biol.* **2014**, *10*, 760−767.
[39] H. Shi, C.-J. Zhang, G. Y. J. Chen, S. Q. Yao, *J. Am. Chem. Soc.* **2012**, *134*, 3001−3014.
[40] K. M. Backus, B. E. Correia, K. M. Lum, S. Forli, B. D. Horning, G. E. González-Páez, S. Chatterjee, B. R. Lanning, J. R. Teijaro, A. J. Oison, D. W. Wolan, B. F. Cravatt, *Nature* **2016**, *534*, 570−574.

10.1002/anie.202105383

[41] S. Pan, S. Y. Jang, S. S. Liew, J. Fu, D. Wang, J. S. Lee, S. Q. Yao, *Angew. Chem. Int. Ed.* **2018**, *57*, 579−583.

[42] D. Mellacheruvu, Z. Wright, A. L. Couzens, J. P. Lambert, N. A. St-Denis, T. Li, Y. V. Miteva, S. Hauri, M. E. Sardiu, T. Y. Low, V. A. Halim, R. D. Bagshaw, N. C. Hubner, A. Al-Hakim, A. Bouchard, D. Faubert, D. Fermin, W. H. Dunham, M. Goudreault, Z. Y. Lin, B. G. Badillo, T. Pawson, D. Durocher, B. Coulombe, R. Aebersold, G. Superti-Furga, J. Colinge, A. J. Heck, H. Choi, M. Gstaiger, S. Mohammed, I. M. Cristea, K. L. Bennett, M. P. Washburn, B. Raught, R. M. Ewing, A. C. Gingras, A. I. Nesvizhskii, *Nat. Methods* **2013**, *10*, 730−736.

[43] a) W.-H. Guo, X. Qi, X. Yu, Y. Liu, C.-I. Chung, F. Bai, X. Lin, D. Lu, L. Wang, J. Chen, L. H. Su, K. J. Nomie, F. Li, M. C. Wang, X. Shu, J. N. Onuchic, J. A. Woyach, M. L. Wang, J. Wang, *Nat. Commun.* **2020**, *11*, 4268; b) R. Gabizon, A. Shraga, P. Gehrtz, E. Livnah, Y. Shorer, N. Gurwicz, L. Avram, T. Unger, H. Aharoni, S. Albeck, A. Brandis, Z. Shulman, B.-Z. Katz, Y. Herishanu, N. London, *J. Am. Chem. Soc.* **2020**, *142*, 11734−11742.

10.1002/anie.202105383

WILEY-VCH

RESEARCH ARTICLE

Entry for the Table of Contents

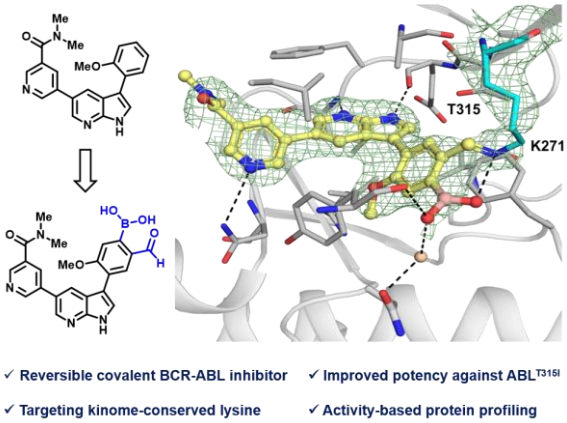

Using iminoboronate chemistry, we report the first successful examples of catalytic lysine-targeting reversible covalent BCR-ABL inhibitors which inhibited both ABL^{WT} and ABL^{T315I} at nanomolar potency. We also demonstrated how the study of off-targets for this class of compounds could be performed using activity-based protein profiling and mass spectrometry.